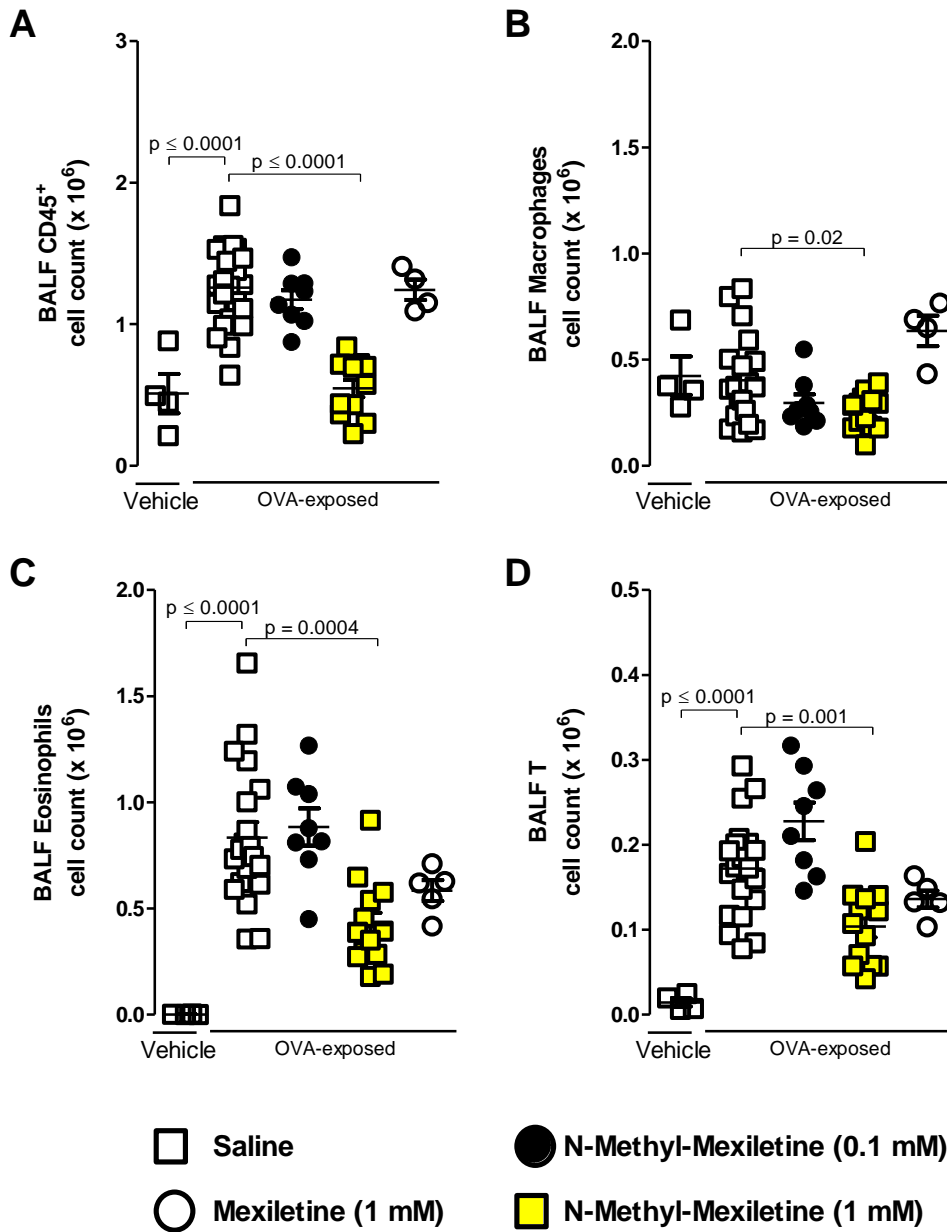
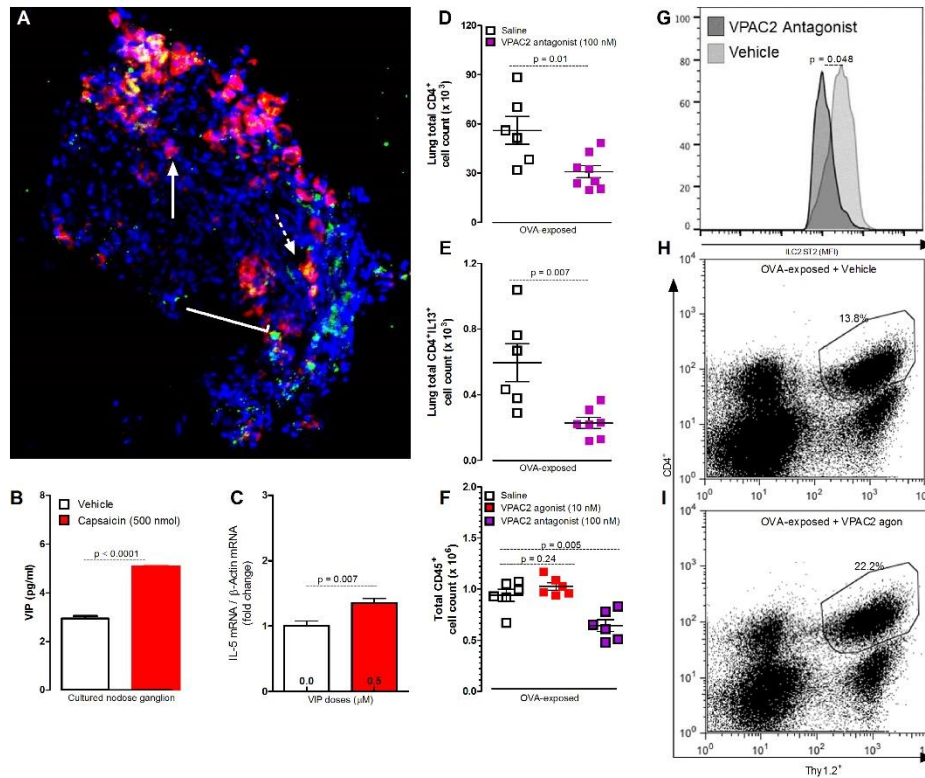


**Figure S1 related to Figure 3: QX-314 abolishes capsaicin-induced peptide neuron activation.** Representative fluorescent microscopy images (scale bar = 10  $\mu$ m) of OVA-challenged mice nodose ganglion sections (20  $\mu$ m) showing phospho-ERK (E, C; yellow) fluorescence in lung afferent neurons (Dil-retrogradely labelled, red) 1 hour after a capsaicin challenge (500 nmol, day 19). Mice pre-treated with QX-314 on day 18; (100  $\mu$ M; C-D) showed fewer phospho-ERK<sup>+</sup> Dil-labelled neurons. Venn diagrams show the total numbers of DAPI (blue), Dil (red) and phospho-ERK (yellow) positive cells in representative nodose ganglion sections from capsaicin exposed OVA-challenge mice pre-treated with saline (A) or QX-314 (C). In the absence of inflammation (E), TRPA1/V1 channels are closed which consequently renders nociceptors refractory to the entry of QX-314. The positive charge present on QX-314 prevents its diffusion through the neuron's lipid bilayer membrane. An exogenous TRP channel opener (e.g. capsaicin (F)) or an asthma-induced inflammatory milieu (G) stimulates TRP channel opening to allow the entry of small charged sodium channel blockers such as QX-314.



**Figure S2 related to Figure 4: Lung sensory neuron silencing with N-methyl-mexiletine decreased OVA-induced allergic inflammation.** OVA challenged mice had increased BALF CD45<sup>+</sup> (A), macrophage (B), eosinophil (C) and T cell (D) counts. Saline or OVA-challenged animals were exposed to N-Methyl-Mexiletine (100-1000  $\mu$ M, nebulized) or mexiletine (1000  $\mu$ M, nebulized) 72h prior to measurement. N-Methyl-Mexiletine (1000  $\mu$ M) significantly decreased BALF leukocytes. Data expressed as mean  $\pm$  S.E.M; *Two-tailed unpaired Student's t-test* (n = 4-12 animals/group; 2 cohorts).



**Figure S3 related to Figure 7: Lung afferents express VIP, and can activate ILC2 and CD4<sup>+</sup> cells via VPAC2.** Representative fluorescent microscopy pictures (A, scale bar = 50  $\mu$ m) of OVA-challenged nodose ganglion sections. Lung afferent neurons were identified by intranasal administration of the retrograde dye Dil 7 days prior sacrifice. Arrow indicates lung afferent (red), L-shape line indicate VIP<sup>+</sup> cells (green) and dot arrow indicates a VIP<sup>+</sup> lung afferent (orange). Cultured nodose ganglion neurons release VIP upon stimulation by capsaicin (500 nmol, red bar) (B) while cultured FACS-sorted CD4<sup>+</sup> cells exposed to VIP (0.5  $\mu$ M, 24h; red bar) display enhanced expression of IL-5 mRNA (C) relative to those treated with vehicle (white bar). Data are expressed as mean  $\pm$  S.E.M; *Two-tailed unpaired Student's t-test* (n = 3 replicate/group; 1 cohort). The VPAC2 antagonist PG 99465 (100 nM, every 12h for 48h starting on day 16; pink squares) diminished OVA-exposed CD4<sup>+</sup> (D), CD4<sup>+</sup>IL5<sup>+</sup> (E) and ILC2 ST2 (IL-33R) MFI (G). The VPAC2 agonist BAY 55-9837 (10nM, every 12h for 96h; red squares) enhanced the relative abundance of CD45<sup>+</sup> (F), CD45<sup>+</sup>Thy1.2<sup>+</sup>CD4<sup>+</sup> cells (H, I), suggesting that VPAC2 contributes to CD4<sup>+</sup> cell polarization. Data expressed as mean  $\pm$  S.E.M; *Two-tailed unpaired Student's t-test* (n = 3-14 animals/group; 1-2 cohorts).

|                 | Control + Vehicle |     |             | Control + QX-314 |                |     | OVA + Vehicle |              |     | OVA + QX-314 |     |   |
|-----------------|-------------------|-----|-------------|------------------|----------------|-----|---------------|--------------|-----|--------------|-----|---|
|                 | Mean              | SEM | N           | Mean             | SEM            | N   | Mean          | SEM          | N   | Mean         | SEM | N |
| Eotaxin (pg/ml) | 1.0 ± 0.8         | 12  | 0.2 ± 0.2   | 12               | 22.7 ± 3.8     | *** | 24            | 5.1 ± 1.7    | +++ | 24           |     |   |
| IL-4 (pg/ml)    | 1.0 ± 0.0         | 12  | 1.0 ± 0.0   | 12               | 2.3 ± 0.2      | *** | 24            | 1.3 ± 0.1    | +++ | 24           |     |   |
| IL-5 (pg/ml)    | 1.0 ± 1.0         | 12  | N.D.        |                  | 389.0 ± 39.2   | *** | 24            | 124.2 ± 21.2 | +++ | 24           |     |   |
| IL-9 (pg/ml)    | 1.0 ± 0.5         | 12  | 0.9 ± 0.4   | 12               | 2.2 ± 0.4      |     | 24            | 0.9 ± 0.3    | +   | 24           |     |   |
| IL-10 (pg/ml)   | 1.0 ± 0.4         | 12  | 0.3 ± 0.2   | 12               | 1.7 ± 0.8      |     | 24            | 0.1 ± 0.1    | +   | 24           |     |   |
| IL-13 (pg/ml)   | 1.0 ± 1.0         | 12  | 10.4 ± 10.4 | 12               | 17.5 ± 10.4    |     | 24            | N.D.         |     |              |     |   |
| IL-17 (pg/ml)   | N.D.              |     | N.D.        |                  | N.D.           |     |               | N.D.         |     |              |     |   |
| IL-23 (pg/ml)   | 1.0 ± 0.1         | 5   | 1.5 ± 0.8   | 4                | 0.6 ± 0.0      | **  | 9             | 0.6 ± 0.0    | **  | 10           |     |   |
| IL-27 (pg/ml)   | 1.0 ± 0.1         | 5   | 0.7 ± 0.1   | 4                | 0.5 ± 0.1      | *   | 9             | 0.6 ± 0.1    | **  | 10           |     |   |
| IL-28b (pg/ml)  | 1.0 ± 0.3         | 5   | 0.5 ± 0.1   | 4                | 0.5 ± 0.1      |     | 9             | 0.5 ± 0.1    |     | 10           |     |   |
| INF-γ (pg/ml)   | 1.0 ± 0.7         | 12  | N.D.        |                  | N.D.           |     |               | 0.1 ± 0.1    |     | 24           |     |   |
| IP-10 (pg/ml)   | 1.0 ± 1.0         | 12  | N.D.        |                  | 1169.3 ± 151.8 | *** | 24            | 198.0 ± 42.1 | +++ | 24           |     |   |
| MCP-1 (pg/ml)   | 1.0 ± 0.4         | 12  | 0.5 ± 0.4   | 12               | 1.3 ± 0.4      |     | 24            | 0.2 ± 0.1    | +   | 24           |     |   |
| RANTES (pg/ml)  | 1.0 ± 0.7         | 12  | N.D.        |                  | N.D.           |     |               | 0.1 ± 0.1    |     | 24           |     |   |
| TNF-α (pg/ml)   | 1.0 ± 0.3         | 12  | 1.2 ± 0.3   | 12               | 1.2 ± 0.2      |     | 24            | 0.3 ± 0.1    | +++ | 24           |     |   |
| TARC (pg/ml)    | 1.0 ± 0.1         | 5   | 1.1 ± 0.3   | 4                | 76.6 ± 22.4    | *   | 9             | 61.2 ± 21.5  |     | 10           |     |   |

**Table S1 related to Figure 5: Lung sensory neuron silencing decrease OVA-induced pro-inflammatory cytokine and chemokine levels in BALF.** Change in BALF level of mediators in CTL and OVA challenged mice exposed to QX-314 (100 μM) or vehicle. Statistical comparisons with the CTL (\*) and OVA challenged mice exposed only to vehicle (†)  $^{*†} P < 0.05$  and  $^{***,+++} P < 0.001$  (n = 4-24 animals/group; 3 cohorts). Data express as mean ± S.E.M; *Two-tailed unpaired Student.*

## **Supplemental Experimental Procedures, related to Experimental procedures.**

### **Animals**

Mice were housed in standard environmental conditions (12-h light/dark cycle; 23°C; food and water ad libitum) at facilities accredited by the Association for Assessment and Accreditation of Laboratory Animal Care. 8-week old BALB/c (stock number: 001026), B6.129P2-Gt26Sortm1(DTA)Lky/J (stock number: 009669) (Voehringer et al., 2008), VIP-Cre (stock number: 001026), LCK-Cre (stock number: 003802), B6.129(Cg)-Gt(ROSA)26Sortm4(ACTB-tdTomato,-EGFP)Luo/J (stock number: 007676) mice were purchased from Jackson Laboratory. Nav1.8 Cre mice were generously supplied by Professor Rohini Kuner (Heidelberg University). We generated a 50/50 percent mixture of Nav1.8-Cre<sup>+/-</sup>DTA<sup>+/-</sup> (Abrahamsen et al., 2008); VIP-Cre<sup>+/-</sup>EGFP/td-tomato<sup>+/-</sup> mice and littermate control (Nav1.8-Cre<sup>-/-</sup>DTA<sup>+/-</sup>; VIP-Cre<sup>-/-</sup>EGFP/td-tomato<sup>+/-</sup>) by crossing male heterozygote Cre mice to female homozygous loxP mice (Voehringer et al., 2008). Mice were used at 8 weeks of age. Offspring were tail clipped; tissue was used to assess the presence of transgene by standard PCR.

### **Drugs**

QX-314 (Binshtok et al., 2007) (Tocris) was diluted in sterile PBS at various concentrations and nebulized for exposure to the mice for 20 min. 1 μmol capsaicin (TRPV1 selective agonist (Caterina et al., 1999), Sigma Aldrich); 10 nM of BAY 55-9837 (VPAC2 selective agonist (Pan et al., 2007), Tocris); 100 nM of PG 99-465 (VPAC2 selective antagonist (Reed et al., 2002), Bachem) or 100 nM of PG 97-269 (VPAC1 selective antagonist (Gourlet et al., 1997), Bachem) were administered intranasally (50 μl volume) to lightly isoflurane-anesthetized mice.

### **Airway hyperresponsiveness**

Deeply anesthetized mice (pentobarbital (60 mg/kg)) underwent a tracheotomy with a 20G sterile catheter. A computer-based analysis of airway hyperresponsiveness was then performed using a Flexivent (SCIREQ) apparatus (Haworth et al., 2008). Mice were ventilated at a tidal volume of 9 ml/kg with a frequency of 150 bpm; positive end-expiratory pressure was set at 2 cm H<sub>2</sub>O. Lung resistance and elastance of the respiratory system was determined in response to in-line aerosolized methacholine challenges (0, 1, 3, 10, 30, 100 mg/ml). Methacholine was dissolved in sterile PBS. The mean elastance and resistance of 10 measurements by doses was calculated.

### **Histology**

Lungs were inflated to 20 cm H<sub>2</sub>O with 1x zinc fixative (BD Pharmigen), the trachea was ligated and lungs stored overnight in zinc fixative (RT, mild shaking). The lungs were then washed in PBS and serially immersed in 30, 50 and 70 % Ethanol solution (20 min/each solution; RT). Tissues were embedded in paraffin, serially cut at 4 μm and stained for hematoxylin and eosin (HE) (Sigma) (Haworth et al., 2008). As described previously (Bilsborough et al., 2008), the level of lung inflammation was assessed, briefly, two blinded investigators scored 384 randomized/scrambled images per condition (6 zones/slide; 4 slides/animal and 3-4 animals/group). The HE score ranges from 0 (absence of inflammatory cells) to 4 (≥5 layers of inflammatory cells in ≥50% bronchioalar submucosa). Moreover, submucosal maximum

membrane thickness (micrometers) was evaluated using a MATLAB (MathWorks software) based computer analysis. Measurements were performed on 160 blinded/scrambled pictures (10 images/animal; 3-4 animals/group).

### **Lung afferent neuron retrograde labelling**

Lung afferent neuron were labelled 1 week prior OVA- or saline- challenge using Dil (Adriaensen et al., 1998) (1,1'-dioctadecyl-3,3',3'-tetramethylindocarbocyanine perchlorhydrate, Molecular Probes). The tracer was applied intra-nasally (2% in PBS, 30  $\mu$ l) in lightly anesthetized mice. Nodose ganglia were harvested on day 21.

### **Immunofluorescence**

Upon harvesting, the nodose ganglia were fixed overnight in 4% para-formaldehyde, washed in PBS and cryoprotected by sequential sucrose immersion (PBS 10-30% sucrose, Overnight). Ganglia were mounted in O.C.T. (Tissue-tek), and serially cut in 20  $\mu$ m coronal sections with a cryostat. The sections were thaw-mounted on Fisherbrad superfrost microscopy slides and kept at -80°C. On the day of the experiment, sections were thawed at room temperature for 10 min. Sections were washed in PBS for 5 min, blocked for 1h at room temperature (PBS, 0.1% Triton X-100, 5% BSA) and exposed to the primary antibodies (Overnight, 4°C), namely rabbit anti-mouse TRPV1 (Alomone, # ACC-030) or rabbit anti-mouse VIP (Novus Biological, # NBP1-78338). Sections were then washed three times in PBS (5 min), exposed to the secondary antibodies (2h, dark), washed, coverslipped with Vectashield (Vector Labs) and observed under confocal microscope (Leica, LSM-710).

### **SYBR green-based quantitative real-time PCR.**

RNA was extracted from primary culture T cells using Qiazol reagent, followed by the RNeasy mini kit (Qiagen, MD). DNase I treatment (Qiagen) was used to remove genomic DNA, and complementary DNA reverse transcribed using Superscript III with random hexamers (Life Technologies). For qPCR, cDNA was subjected to 2-step thermocycling using fast SYBR green master mix (Life Technologies), and data collection performed on an Applied Biosystems 7500 machine (Life Technologies). Expression levels were normalized to  $\beta$ -actin using the  $\Delta\Delta$ Ct method. The primers used in this study were  $\beta$ -actin forward: TCG TAC CAC AGG CAT TGT GAT GGA;  $\beta$ -actin reverse: TGA TGT CAC GCA CGA TTT CCC TCT, Interleukin-4 forward: AGATGGATGTGCCAAACGTCCTCA; Interleukin-4 reverse: AATATGCGAAGCACCTTGGGAAGCC; Interleukin-5 forward: GCTTCCTGTCCCTACTCATAAA, Interleukin-5 reverse: CCCACGGACAGTTTGATTCT, Interleukin-13 forward: CAGCAGCTTGAGCACATTTC and Interleukin-13 reverse: CGGGATACTGACAGACTCATTT.

### **Bronchoalveolar lavage (BAL)**

On day 21, mice were anesthetized following an intraperitoneal injection of urethane (200  $\mu$ l i.p., 35%) and a 20G sterile catheter inserted longitudinally into the trachea. 2 ml of ice cold PBS containing protease inhibitors (Roche) was injected into the lung, harvested and stored on ice. BAL fluid underwent a 400g centrifugation (15 min; 4°C), the supernatant was discarded and cells resuspended in 200  $\mu$ l (Haworth et al., 2008).

### **Airway inflammatory and differential cell count**

Bronchoalveolar lavage fluid (BALF) cells were resuspended in FACS buffer (PBS, 2% FCS, EDTA), and incubated with Fc block (0.5 mg/ml, 10 min; BD Biosciences). Cells were then stained with monoclonal antibodies (FITC anti-mouse CD45, BD Biosciences, cat no: 553079, PE anti-mouse Siglec-F, BD Biosciences, cat no: 552126; APC anti-mouse GR-1, eBiosciences, cat no: 17-5931-81; PE-Cy7 anti-mouse CD3e, cat no: 25-0031-81; PerCP anti-mouse F4/80, BioLegend, cat no: 123125; PE anti-mouse, BD Bioscience, cat no: 552126; 45 min, 4°C on ice) before data acquisition on a FACS Canto II (BD Biosciences). A leukocyte differential count was determined during flow cytometry analysis of cells expressing the common leukocyte antigen CD45 (BD Pharmigen; cat no: 553079). Specific cell populations were identified as follows: macrophages as F4/80<sup>Hi</sup>-Ly6g<sup>Neg</sup>, eosinophils as F4/80<sup>Int</sup>-Ly6g<sup>Lo</sup>-Siglec<sup>F</sup><sup>Hi</sup>, neutrophils as F4/80<sup>Lo</sup>-Ly6g<sup>Hi</sup>-Siglec<sup>F</sup><sup>Neg</sup>, and lymphocytes as F4/80<sup>Neg</sup>-Ly6g<sup>Neg</sup>-CD3<sup>Pos</sup>. Total BAL cell counts were performed using a standard hemocytometer, with absolute cell numbers calculated as total BAL cell number multiplied by the percentage of cell subpopulation as determined by FACS (Haworth et al., 2008).

### **ILC gating strategy**

A single cell suspension was prepared from lung tissue and ILCs were identified flow cytometry using a tiered gating strategy. Cells were first identified using light scatter parameters (FSC by SSC) and doublets were excluded using FSC-Area by FSC-Height. Live hematopoietic cells were then identified by gating on CD45<sup>+</sup> 7AAD<sup>-</sup> cells. This population was then assessed for Thy1 expression and the Thy1<sup>+</sup> population was further analyzed for expression of canonical, lineage defining myeloid (CD11b/CD11c/Gr1) or lymphoid (CD3/CD4/CD8/TCR $\beta$ /CD19/NK1.1/TCR $\gamma$ / $\delta$ ) markers and a gate drawn on Lin<sup>-</sup> Thy1<sup>+</sup> cells. The majority of cells falling in this Lin<sup>-</sup> Thy1<sup>+</sup> gate expressed high levels of IL-7R $\alpha$ , typical of ILCs. Within this population, ILC2s could further be identified as Lin<sup>-</sup>Thy1<sup>+</sup>ST2<sup>+</sup>CD25<sup>Hi</sup>, consistent with the previously published reports (Monticelli et al., 2011).

### **Intracellular Cytokine Staining**

Cells were stimulated with PMA/Ionomycin in the presence of GolgiPlug (BD Biosciences) for 4 hours and then fixed and stained using the BD Cytofix/Cytoperm kit following manufacturer's instructions (BD Biosciences).

### **T Cell Culture and Isolation**

Mouse CD4<sup>+</sup> T cells were isolated from spleen and peripheral nodes and differentiated into different subsets as previously described (De Jager et al., 2009). Briefly, tissues were mashed through 70 $\mu$ m mesh and CD4 T cells purified with anti-CD4 mAb coated magnetic beads per manufacturer's instructions (Miltenyi Biotec). Cells were then activated on tissue culture plates that had been coated with anti-CD3/anti-CD28 each at a concentration of 2  $\mu$ g/ml, along with cytokines appropriate for differentiation into the desired subset. For T<sub>H</sub>2 cultures, cells were activated in the presence of 40 ng/ml of IL-4, while for T<sub>H</sub>1 differentiation they were activated in the presence of 10 ng/ml of IL-12, and for T<sub>H</sub>17 differentiation they were activated with 30 ng/ml of IL-6 and 3 ng/ml of TGF- $\beta$ . Cultures were removed from the anti-CD3/CD28 stimulation and fresh media was added after 48 hours. Cultures were monitored daily by microscopy and once cells were observed to be entering a resting state they were re-stimulated

on tissue culture plates coated with anti-CD3/CD28 in the presence of the indicated concentration of mouse recombinant VIP for 48 hours (R&D).

### **T cell proliferation**

CD4<sup>+</sup> T cells were purified from spleens of C57Bl/6 mice using CD4 microbeads (L3T4, Miltenyi Biotec). Purified cells were stained with Cell Trace Proliferation Kit (Invitrogen). 96 u-shaped plates were coated with anti-CD3 (1 µg/ml, Biolegend) with anti-CD28 (1 µg/ml, Biolegend) in PBS for 3 hours at 37°C. T cells were plated at 105 cells/well and appropriate concentration of QX-314 was added in IMDM+PenStrep+Lgly+10% FCS. Alternatively, the cells were cultured for 24 hours and expression of activation marker CD62L was analyzed using Flow Cytometry and the supernatant was collected in which IL-2 concentration was measured using an ELISA kit (Sonner et al.) (Biolegend) or the cells were cultured for 3 days and proliferation was assayed by FACS cytometry on viable cells.

### **T cell differentiation**

CD4<sup>+</sup> T cells were purified from spleens of C57Bl6 mice using CD4 microbeads (L3T4, Miltenyi Biotec) and stimulated with plate-bound anti-CD3 (2 µg/ml) and anti-CD28 (2 ug/ml) plus recombinant murine IL-4 (10 ng/ml, Biolegend) and anti-IL-12 (20 µg/ml, Biolegend). After 48 hours the cells were split and cultured in recombinant murine IL-2 (10 ng/ml, Biolegend) for an additional 4-5 days. Alternatively, (1) cells were stimulated with PMA, ionomycin and Golgi plug for 4 hrs. Cells were harvested, washed and fixed and intra-cellularly stained for IL-4 and IL-17, and analyzed on a Flow cytometer (Sonner et al.); cells were harvested, washed and re-seeded at 105 cells/well on CD3/28 coated wells for 48hrs. Supernatant was collected and IL-4 was measured using an ELISA kit (Biolegend).

### **Eosinophil and Macrophage functions**

OVA-challenged mice (day 14-17) were sacrificed on day 18 and BALF harvested. Macrophages (F4/80Hi-Ly6gNeg) and eosinophils (F4/80Int-Ly6gLo-SiglecFHi) were immunophenotyped using FACS-sorting and harvested in ice-cold DMEM (20% FBS).

### **Chemotaxis**

Macrophages and eosinophils (0.1M/well) were seeded in the top well of 3 µm (eosinophils) and 5 µm (macrophages) pore transwell (Corning) plate (Palframan et al., 1998). Recombinant mouse Eotaxin-2 (Palframan et al., 1998) (25 ng/ml, 4h; Peptrotech) or CCL-2 (Murdoch et al., 2004) (25 ng/ml, 43h; Peptrotech) was co-applied with QX-314 (0-1.0%) in the transwell lower chamber. Numbers of cells that migrated to the bottom chamber were measured using a standard hemocytometer to assess chemotactic function of the cells.

### **Survival and activation**

Macrophages and eosinophils (0.1M/well) were put in culture and exposed to LPS (50 ng/ml) or vehicle for 24h in the presence of QX-314 (0.1-1.0%) or saline. Total cell count was measured using a standard hemocytometer and survival expressed as number of dead cells per total cell count. To monitor eosinophil and macrophage activation we measured the release of IL-1β in the supernatant using standard ELISA (eBioscience, cat no: 88-7013-88).



## **ELISA**

BALF supernatant volumes were concentrated to a final 200 µl volume following a 3h RT SpeedVac (Thermo Scientific; SpeedVac Concentrator, SPD1010) cycle. Samples were processed using commercial ELISA kit specifically designed for VIP (Phoenix Pharmaceuticals; catalog number EK-064-16).

## **Microarray analysis**

As previously described by our laboratory (Chiu et al., 2013), total RNA was extracted by sequential Qiazol extraction and purification through the RNeasy micro kit with on column genomic DNA digestion (Qiagen). RNA quality was determined by an Agilent 2100 Bioanalyzer using the RNA Pico Chip (Agilent). RNA was amplified into cDNA using the Ambion wild-type expression kit for whole transcript expression arrays, with Poly-A controls from the Affymetrix Genechip Eukaryotic Poly-A RNA control kit. The Affymetrix Genechip WT terminal labelling kit was used for fragmentation, biotin labelling. Affymetrix GeneChip Hybridization control kit and the Affymetrix GeneChip Hybridization, wash, stain kit was used to hybridize samples to Affymetrix Mouse Gene ST 1.0 GeneChips, fluidics performed on the Affymetrix Genechip Fluidics Station 450, and scanned using Affymetrix Genechip Scanner 7G (Affymetrix).. Affymetrix CEL files were normalized with the robust multi-array average (RMA) algorithm with quantile normalization, background correction, and median scaling. Nociceptor microarray data sets are deposited at the GEO database under accession number GSE46546 (Chiu et al., 2013).

## **Neuronal cultures and calcium imaging**

Adult mice (8 weeks) were sensitized (day 0, 7) and challenged (day 14-17) with ovalbumin and nodose ganglia (day 21) were dissected out into DMEM medium (Life Technologies, CA, USA), completed with 50 U/mL penicillin and 50 µg/mL Streptomycin (Fisher, # MT-3001-CI), 2mM L-Glutamine (Life Technologies, # 25030-081) and 10% HI FBS (Life Technologies, # 10082-145). Cells were then dissociated in HEPES buffered saline (Sigma, MO, USA) (completed with 1 mg/mL Collagenase A + 2.4 U/mL dispase II (enzymes, Roche Applied Sciences, IN, USA) and incubated for 70 minutes at 37°C. Ganglions were triturated with glass Pasteur pipettes of decreasing size in Neurobasal-A medium (2% B27 supplement), then centrifuged over a 10% BSA gradient in PBS, plated on Poly-D-Lysine coated cell culture dishes. Cells were cultured with Neurobasal-A medium (completed with 0.05 ng/µL NGF (Life Technologies, # 13257-019), 0.002 ng/µL GDNF (Sigma, # G1401), 0.01 mM AraC (Sigma, # C6645) and 10% HI FBS (Life Technologies 10082-145) and used for calcium imaging and electrophysiology 16-48 hours post-plating.

For calcium imaging, cells were loaded with 10 µM Fura-2-AM (Life Technologies) at 37°C for 30-45 min in Neurobasal-A medium, washed into Standard Extracellular Solution (SES, 145 mM NaCl, 5 mM KCl, 2 mM CaCl<sub>2</sub>, 1 mM MgCl<sub>2</sub>, 10 mM glucose, 10 mM HEPES, pH 7.5), and imaged at room temperature. Cells were illuminated by an UV light source (Xenon lamp, 75 watt, Nikon, NY, USA), 340 nm and 380 nm excitation alternated by a LEP MAC 5000 filter wheel (Spectra services, NY, USA), and fluorescence emission captured by Cool SNAP ES camera (Princeton Instruments, NJ, USA). 340/380 ratiometric images were processed, background corrected, and analyzed with IPLab software (Scientific Analytics, CA, USA). Microsoft Excel was used for further analyses (Microsoft, USA). Ligands were flowed (15s) directly onto neurons using perfusion barrels followed by buffer washout (1min45s minimum) and further application. Mouse

recombinant IL-5 (Peprotech, # 215-15), IL-13 (Peprotech, # 210-13) and Eotaxin-2 (Peprotech, # 250-22) were prepared in SES at concentration from 0-10  $\mu\text{g}/\text{ml}$ . In some experiments, 1  $\mu\text{M}$  capsaicin (Tocris), 100  $\mu\text{M}$  AITC (Sigma) or 40 mM KCl (Sigma) was applied following the cytokines.

### **Current clamp recordings**

48 hours after plating, only small cells (<45 pF) that responded to IL-5 in calcium imaging experiment were recorded in whole-cell mode. A multiclamp 700B amplifier, digidata 1440a digitizer and clampex software (Molecular Devices) were used for recordings. Data were sampled at 10 kHz. Pipettes were pulled from thick-walled borosilicate glass capillaries on a Sutter Instruments P-97 and had a resistance < 3 M $\Omega$ , when filled with the pipette solution. Capacity transients were canceled and series resistance was compensated of around 90%. After obtaining whole-cell configuration, cells were held at -60 mV for 3 min to allow equilibrium, and only cells that had stable and low access resistance (generally 5 M $\Omega$ , always < 10 M $\Omega$ ) throughout the whole protocol were analyzed. Resting membrane potential (RMP) was obtained by averaging 1 minute of recording once the cell was stable. IL-5 perfusion took from 30 s to 1 min to reach maximum effect, and average of 20 seconds recording of the RMP was made after apparent maximum effect of IL-5. Time for washout was very long (> 15 min), and thus only 3 cells (out of 12) underwent complete washout. Control was also performed where cells were recorded for 5 minutes and were not perfused with IL-5. These cells did not exhibit modification of their RMP (n = 5 cells). Series of 5 ms depolarizing steps (25 pA increment) were applied as to determine the current necessary to elicit action potential (defined as rheobase). Only cells that had a delta of 60 mV between the threshold and the maximum peak amplitude of the action potential were analyzed. Depolarizing ramp currents (600 and 1200 pA for 500 ms) were applied to examine spiking frequency. Membrane potential was corrected for liquid junction potential (-15 mV). Pipette solution contained the following in mM: K gluconate, 135; KCl, 10; MgCl<sub>2</sub>, 1, EGTA, 5; HEPES, 10 (300 mOsm, and pH = 7.3). Standard external solution was obtained from Boston BioProducts and contained the following in mM: NaCl, 145; KCl, 5; CaCl<sub>2</sub>, 2; MgCl<sub>2</sub>, 1; Glucose, 1; HEPES, 10 (pH = 7.4).

### **Assessment of the distance travelled during free access to running wheels**

Voluntary wheel running was assessed as described (Cobos EJ). Briefly, mice were put in polycarbonate cages (20.5 cm wide  $\times$  36.5 cm long  $\times$  14 cm high) with free access to stainless steel activity wheels (diameter 23 cm; width 5 cm) with a ball-bearing axle (Bioseb, Boulogne, France). The wheel could be turned in either direction. Multiple activity cages were contained within a testing room. The wheels were connected to a computer that automatically recorded the distance, number of bouts, average acceleration and average speed were recorded for each animal. No experimenters were present in the room during the evaluation sessions. Mice were habituated in individual activity cages for three sessions over at least seven days. In the first habituation session, each mouse was randomly assigned to a specific cage in which they were always tested for the duration of the experiment. Voluntary exercise was monitored daily throughout the allergen sensitization (day 0, 7) and challenge (day 14-17) protocol. The distance traveled was compared between the pre-allergen challenge period (day 13), at the peak of inflammation and prior QX-314 treatment (day 18) and 1 day following QX-314 treatment (day 19).

## **Supplemental References.**

Abrahamsen, B., Zhao, J., Asante, C.O., Cendan, C.M., Marsh, S., Martinez-Barbera, J.P., Nassar, M.A., Dickenson, A.H., and Wood, J.N. (2008). The cell and molecular basis of mechanical, cold, and inflammatory pain. *Science* 321, 702-705.

Adriaensen, D., Timmermans, J.P., Brouns, I., Berthoud, H.R., Neuhuber, W.L., and Scheuermann, D.W. (1998). Pulmonary intraepithelial vagal nodose afferent nerve terminals are confined to neuroepithelial bodies: an anterograde tracing and confocal microscopy study in adult rats. *Cell Tissue Res* 293, 395-405.

Bilsborough, J., Chadwick, E., Mudri, S., Ye, X., Henderson, W.R., Jr., Waggle, K., Hebb, L., Shin, J., Rixon, M., Gross, J.A., and Dillon, S.R. (2008). TACI-Ig prevents the development of airway hyperresponsiveness in a murine model of asthma. *Clin Exp Allergy* 38, 1959-1968.

Binshtok, A.M., Bean, B.P., and Woolf, C.J. (2007). Inhibition of nociceptors by TRPV1-mediated entry of impermeant sodium channel blockers. *Nature* 449, 607-610.

Caterina, M.J., Rosen, T.A., Tominaga, M., Brake, A.J., and Julius, D. (1999). A capsaicin-receptor homologue with a high threshold for noxious heat. *Nature* 398, 436-441.

Chiu, I.M., Heesters, B.A., Ghasemlou, N., Von Hehn, C.A., Zhao, F., Tran, J., Wainger, B., Strominger, A., Muralidharan, S., Horswill, A.R., *et al.* (2013). Bacteria activate sensory neurons that modulate pain and inflammation. *Nature* 501, 52-57.

De Jager, P.L., Baecher-Allan, C., Maier, L.M., Arthur, A.T., Ottoboni, L., Barcellos, L., McCauley, J.L., Sawcer, S., Goris, A., Saarela, J., *et al.* (2009). The role of the CD58 locus in multiple sclerosis. *Proc Natl Acad Sci U S A* 106, 5264-5269.

Gourlet, P., De Neef, P., Cnudde, J., Waelbroeck, M., and Robberecht, P. (1997). In vitro properties of a high affinity selective antagonist of the VIP1 receptor. *Peptides* 18, 1555-1560.

Haworth, O., Cernadas, M., Yang, R., Serhan, C.N., and Levy, B.D. (2008). Resolvin E1 regulates interleukin 23, interferon-gamma and lipoxin A4 to promote the resolution of allergic airway inflammation. *Nat Immunol* 9, 873-879.

Monticelli, L.A., Sonnenberg, G.F., Abt, M.C., Alenghat, T., Ziegler, C.G., Doering, T.A., Angelosanto, J.M., Laidlaw, B.J., Yang, C.Y., Sathaliyawala, T., *et al.* (2011). Innate lymphoid cells promote lung-tissue homeostasis after infection with influenza virus. *Nat Immunol* 12, 1045-1054.

Murdoch, C., Giannoudis, A., and Lewis, C.E. (2004). Mechanisms regulating the recruitment of macrophages into hypoxic areas of tumors and other ischemic tissues. *Blood* 104, 2224-2234.

Palframan, R.T., Collins, P.D., Williams, T.J., and Rankin, S.M. (1998). Eotaxin induces a rapid release of eosinophils and their progenitors from the bone marrow. *Blood* 91, 2240-2248.

Pan, C.Q., Li, F., Tom, I., Wang, W., Dumas, M., Froland, W., Yung, S.L., Li, Y., Roczniak, S., Claus, T.H., *et al.* (2007). Engineering novel VPAC2-selective agonists with improved stability and glucose-lowering activity in vivo. *J Pharmacol Exp Ther* 320, 900-906.

Reed, H.E., Cutler, D.J., Brown, T.M., Brown, J., Coen, C.W., and Piggins, H.D. (2002). Effects of vasoactive intestinal polypeptide on neurones of the rat suprachiasmatic nuclei in vitro. *J Neuroendocrinol* 14, 639-646.

Sonner, J.M., Antognini, J.F., Dutton, R.C., Flood, P., Gray, A.T., Harris, R.A., Homanics, G.E., Kendig, J., Orser, B., Raines, D.E., *et al.* (2003). Inhaled anesthetics and immobility: mechanisms, mysteries, and minimum alveolar anesthetic concentration. *Anesthesia and analgesia* 97, 718-740.

Voehringer, D., Liang, H.E., and Locksley, R.M. (2008). Homeostasis and effector function of lymphopenia-induced "memory-like" T cells in constitutively T cell-depleted mice. *J Immunol* 180, 4742-4753.